Available online at www.sciencedirect.com
ScienceDirect
Journal of Food Engineering 79 (2007) 1269–1279
JOURNAL OF FOOD ENGINEERING
www.elsevier.com/locate/jfoodeng

Microwave driven convection in a rotating cylindrical cavity: A numerical study

Sourav Chatterjee [a], Tanmay Basak [b], Sarit K. Das [a,*]

[a] Department of Mechanical Engineering, Indian Institute of Technology, Madras, Chennai 600036, India
[b] Department of Chemical Engineering, Indian Institute of Technology, Madras, Chennai 600036, India

Received 11 November 2005; accepted 11 April 2006
Available online 7 May 2006

Abstract

The heating of containerized liquid using microwave radiation is investigated numerically. The numerical model is validated with an earlier experimental study. Unlike previous studies, the turntable rotation is taken into account. The effects of turntable rotation, natural convection, power sources, and aspect ratio of container on the temperature profiles are studied. Detailed results of temperature profiles, stream functions and time evolution of flow field are presented. An attempt is made to physically explain the complex flow pattern due to the effects of rotational and gravitational forces and spatially non-uniform internal heat generation typical in microwave heating. A correlation, for the transient changes of temperature is arrived at. Current studies indicate that turntable rotation does not aid in achieving uniform heating in case of a symmetric heat source.

Keywords: Microwave heating; Natural convection; Rotation; Heat generation; Lambert's law; Numerical modeling

1. Introduction

Microwave heating is a process common to many industrial and household applications. Brief startup times, internal heating, high energy efficiency and less process time have made it an attractive alternative over conventional heating methods. One of its principal advantages is that, unlike conventional heat sources, it does not simply provide heat externally to the surface of the body, but the irradiation penetrates the surface and produces considerable internal volumetric heating, thus leading to a greater uniformity of temperature in the heated body. The technology has several important applications, the most notable being the domestic microwave oven. It is also used in the food industry for pasteurization, sterilization, freeze-drying etc. Other uses include ceramic processing (Sutton, 1989), curing of epoxy resins (Le Van & Gourdenne, 1987) and process adhesives (Malaczynski, 1988).

Although there is a large amount of literature relating to the modeling of microwave heat transfer, most of the studies have concentrated on solids. Little efforts have been concentrated on the modeling of microwave heat transfer on containerized liquids, especially a detailed study of the parameters affecting such heating and the flow patterns accompanying it. This is because of the complex power distributions inside the cavity, and its highly coupled and complicated effects on the flow field, which makes a straightforward analytical solution impossible.

In microwave heating of liquids, a non-uniform volumetric heat source causes spatial variation in temperature which leads to buoyancy driven convective flow. The earliest studies, for example, Lenz (1980), have used a lumped parameter approach in modeling microwave heating of liquids. But Datta, Prosetya, and Hu (1992) illustrated, that significant temperature variations can be observed due to the buoyancy driven heating. Datta et al. (1992) used the Lambert's law to model the volumetric heat source and

* Corresponding author. Tel.: +91 44 2257 4655.
E-mail address: skdas@iitm.ac.in (S.K. Das).

0260-8774/$ - see front matter © 2006 Elsevier Ltd. All rights reserved.
doi:10.1016/j.jfoodeng.2006.04.039

Nomenclature

E_0	electric field at surface	τ	non-dimensional time
Ez	electric field at a distance 'z' from the surface	θ	non-dimensionalised temperature
a	attenuation constant	t_{max}	maximum simulation time
b	phase constant	ρ	density of the fluid
Q_0	rate of heating at the surface	c_p	specific heat at constant pressure
Q	rate of heating	q	dimensionless power
z	azimuthal co-ordinate	Pr	Prantdl number
R	radius of the vessel	$\hat{i}$	radial direction
r	radial co-ordinate	$\hat{k}$	azimuthal direction
δ	penetration depth	Ω	angular velocity
f	frequency of microwaves	h	height of the cylinder
ε_o	dielectric constant of vacuum	υ	kinematic viscosity
ε''	dimensionless relative dielectric loss of material	Ta	Taylor number
λ_o	wavelength of the microwaves at free space	Ra	internal Rayleigh number
ε'	dimensionless relative dielectric constant of material	Ra_r	rotational Rayleigh number
		Fr	Froude number
T	temperature	τ_{max}	non-dimensional maximum simulation time
T_0	initial temperature	g	gravitational acceleration
$\bar{r}$	non-dimensional radial distance	β	coefficient of thermal expansion of the fluid
$\overline{V}$	non-dimensional velocity vector of a fluid particle	w	Swirl velocity
		R^2	coefficient of determination
α	thermal diffusivity	A	aspect ratio (R/h)

analyzed the temperature profiles on the heating of a containerized liquid. A study of microwave induced natural convection was made by Zhang, Jackson, and Ungan (2000). The model solved the Maxwell's equation in 3D using the FDTD method and solved the flow field for distilled water and corn oil. An FDTD solution was also employed by Ratanadecho, Aoki, and Akahori (2002) for microwave heating using a rectangular wave guide. Ayappa, Brandon, Derby, Davis, and Davis (1994) used finite element methods to study the convections in a square cavity exposed to waves from different directions. Finite element method was also employed by Basak and Ayappa (2001) to study the importance of natural convection in microwave thawing. However, except in the studies by Basak and Ayappa (2001), the flow physics was not exhaustively brought out and the effects of different parameters on the flow physics were not presented in detail.

Natural convection, in the presence of volumetric heat sources have been studied in detail by May (1991), Roschina, Uvarov, and Osipov (2005), Tasaka and Takeda (2005) etc. Tasaka and Takeda (2005) studied the effect of an exponential heating source on Rayleigh Benard convection. However, the system in this case, was stationary.

The significant contribution in the present study is natural convection under the effect of rotational forces. Convection in rotating cavities has been extensively studied in literature. The works of Boubnov and Golitsyn (1986), Hamady, Lloyd, Yang, and Yang (1994), Hudson, Tang, and Abell (1978) and Rossby (1969) may be cited as examples. A detailed discussion on the effect of rotation on natural convection can be found in Boubnov and Golitsyn (1995). However, such cases do not involve a spatially non-uniform volumetric heat generation.

The combination of internal heat generation and rotating effects makes the present problem unique and applicable to microwave heating of liquid inside rotating container. An exhaustive study of the flow field in such a complex situation is, to the best of our knowledge, yet to appear in literature.

The objective of the study is to analyze, by a numerical investigation, the effect of the various parameters, namely the rotational forces, power source intensity and the gravitational forces, on the microwave heating of containerized liquids in the presence of rotating turntables.

2. Mathematical model

The cylindrical sample is assumed to be incident with microwaves which are radially symmetrical as shown in Fig. 1. We have considered both the stationary and rotating cases. Mathematical modeling of microwave heating involves two discrete, but coupled parts, the determination of the electromagnetic field at a particular point, and a complete solution of the flow field and temperature fields at that point.

2.1. Electromagnetic field

An exact description of the electromagnetic field at a point is given by the Maxwell's equation. The heating in

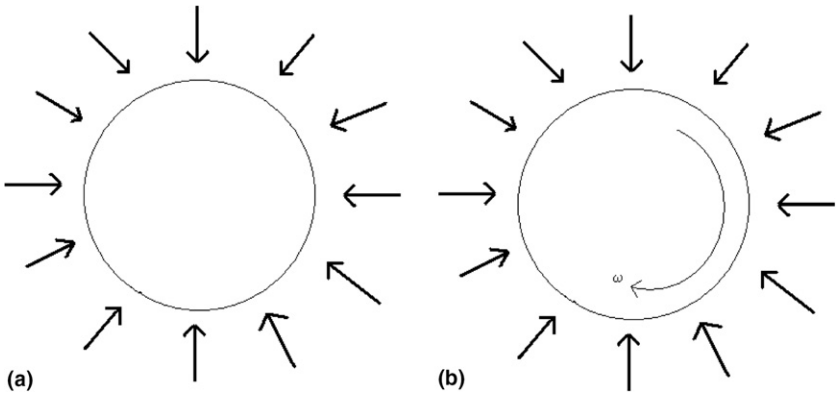

Fig. 1. Top view of cylinder with radially symmetric microwave radiation incident on it (a) static case and (b) rotating case.

a microwave oven takes place by the dissipation of the energy stored in the electromagnetic field at each point. Thus, an exact solution would involve the numerical solution of the Maxwell's equation at each point. This has been attempted in various previous studies. This is more involved and it has not been attempted to go into such complexities since the electric field in our case lends itself to simpler interpretation. As we know, in the special case of a semi-infinite slab, there exists a simple analytical solution to the Maxwell's equation (Saltiel & Datta, 1999)

$$Ez = E_0 \exp(-az)\exp(-jbz) \tag{1}$$

where '*a*', the attenuation constant, controls the rate at which the incident field decays, and '*b*', the phase constant representing a phase change.

Consequently, the power distribution can be expressed as

$$Q = Q_0 \exp\left(\frac{-z}{\delta}\right) \tag{2}$$

Here, δ represents the penetration depth, the distance at which the energy falls to e^{-1} of its value at the material surface. This functional form of the power expression is the so called Lambert's law. The Lambert's law can however be successfully used to predict the power generation in more practical cases. Studies by Ayappa, Davis, Crapiste, Davis, and Gordon (1991) verify this. The Lambert Law formulation has been successfully used by Datta et al. (1992) in case of containerized liquids and Wei, Davis, Davis, and Gordon (1985) in case of porous materials. Based on these works, it may be noted that the scheme is found to give a good approximation to the Maxwell's Equation in cases where the depth is large.

However, it is important to note that the Lambert's law does not take into account standing wave patterns formed in the cavity and hence, do not give agreeable results in case of containers of small radius due to focusing effects (Prosetya & Datta, 1991), especially near the outer boundary (Yang & Gunasekaran, 2004). In our case of a cylindrical enclosure, the Lambert's law leads to

$$Q = Q_0 \exp\left[\frac{-(R-r)}{\delta}\right] \tag{3}$$

where

$$Q_0 = 2\pi f \varepsilon_0 \varepsilon'' E_0^2 \tag{4}$$

$$\text{and} \quad \delta = \left[\frac{\lambda_0}{2\pi(2\varepsilon')^{1/2}}\right]\left(\sqrt{1+\left(\frac{\varepsilon''}{\varepsilon'}\right)^2}-1\right) \tag{5}$$

We have considered the temperature dependence of the dielectric properties as in Datta et al. (1992). The temperature dependence leads to a change in the penetration depth with increase in temperature. The depth can be approximated as a linear function of temperature, as in Datta et al. (1992).

The function, in the range of 20 °C and 55 °C is given as

$$\delta = 0.004408 + 0.0005752T \tag{6}$$

In Eq. (6), the temperature is in °C and the depth is in metres.

2.2. Fluid flow and heat transfer

The fluid flow is obtained by solving the continuity and the Navier–Stokes equation. The heat transfer to the fluid is modeled by the energy equation. The equations have been non-dimensionalised using the following non-dimensional parameters:

$$\bar{r} = r/h, \quad \overline{V} = Vh/\alpha, \quad \tau = \alpha t/h^2,$$
$$\theta = (T - T_0)/(Q_0 t_{\max}/\rho c_p), \quad q = Q_0 t_{\max}/\rho c_p T_0 \tag{7}$$

In the 2D-axisymmetric case, the equations are given as follows:

Continuity equation:

$$\nabla \overline{V} = 0 \tag{8}$$

The momentum equation:

$$\frac{1}{Pr}\left[\frac{\partial \overline{V}}{\partial t} + (\overline{V}.\nabla)\overline{V}\right] = \Delta\overline{V} + (Ra_r\hat{i} - Ra\hat{k})\theta - 2(Ta)^{1/2}(\hat{k}\times\overline{V}) \tag{9}$$

where

$$\Delta\overline{V} = \frac{1}{\bar{r}}\frac{\partial}{\partial\bar{r}}\left(\bar{r}\frac{\partial\overline{V}}{\partial\bar{r}}\right) + \frac{\partial^2\overline{V}}{\partial\bar{z}^2} \tag{10}$$

The non-dimensional parameters involved in this equation are

Taylor number:

$$Ta = \frac{\Omega^2 h^4}{\nu^2} \tag{11}$$

Rayleigh number:

$$Ra = \frac{g\beta Q_0 t_{\max} h^3}{\rho c_p \alpha \nu} \tag{12}$$

Rotational Rayleigh number:

$$Ra_r = \frac{\Omega^2 R\beta Q_0 t_{\max} h^3}{\rho c_p \alpha \nu} \tag{13}$$

Taylor number is the ratio of the rotational and viscous forces. The Rayleigh number is the ratio of buoyancy and the viscous forces. Since the flow is not driven by a temperature gradient, but by an internal heat generation, we cannot define an external Rayleigh number. Hence, the Rayleigh number defined here is an internal Rayleigh number.

Energy equation:

$$\frac{\partial \theta}{\partial t} + (\overline{V}.\nabla)\theta = \Delta\theta + \frac{\exp\left(\frac{(r-R)}{\delta}\right)}{\tau_{\max}} \tag{14}$$

where $\tau_{\max}$ is the non-dimensionalised maximum time and

$$\Delta\theta = \frac{1}{\overline{r}}\frac{\partial}{\partial \overline{r}}\left(\overline{r}\frac{\partial \theta}{\partial \overline{r}}\right) + \frac{\partial^2 \theta}{\partial \overline{z}^2} \tag{15}$$

The fluid is assumed to be incompressible except that the effect of variable density in the buoyancy term in the momentum equation is accounted for by using the Boussinesq approximation. The Boussinesq approximation is written as

$$\rho_0 - \rho = \rho\beta(T - T_0) \tag{16}$$

In case of a static container, the boundary and initial conditions are the same as those used by Datta et al. (1992). There is a no slip boundary conditions at the side walls and at the top and bottom which implies

$$u = 0 \quad \text{at } z = 0, h \tag{17}$$

$$v = 0 \quad \text{at } r = R \tag{18}$$

In case of a rotating flow, with respect to a static frame, no slip at the walls also implies

$$w = \Omega R \quad \text{at } r = R \tag{19}$$

The walls of the container are taken to be thermally insulated, and hence the heat flux through them is zero. This translates to

$$\partial T/\partial z = 0 \quad \text{at } z = 0, h \tag{20}$$

$$\partial T/\partial r = 0 \quad \text{at } r = R \tag{21}$$

Further, we have assumed axisymmetry which imposes the constraint

$$\partial T/\partial r = 0 \quad \text{and} \quad \partial u/\partial r = 0 \quad \text{at } r = 0 \tag{22}$$

$$\partial \phi/\partial \theta = 0 \quad \text{everywhere} \tag{23}$$

where ϕ is any flow property.

The initial conditions used are

$$T = 25\ ^\circ\text{C}, \quad u = 0, \quad v = 0 \tag{24}$$

3. Numerical solution

The heat transfer and fluid flow equations were solved by using the commercially available software FLUENT where the finite volume method is used to discretise and solve the flow and energy equations. The microwave power was modeled by writing a user defined function, which was appended to the FLUENT code. The flow was assumed to be laminar, and an axisymmetric solver was used. The mass and momentum equations were solved using a first order implicit method in space and time.

Flow and energy equations were solved with a first order upwind scheme for momentum and energy discretisations. Pressure interpolation was done using the PRESTO method. The PRESTO method is highly effective in case of buoyancy driven flows as well as for rotating flows. Since the flows encountered in our case had both these characteristics, the PRESTO method was found to be the best. Pressure–velocity coupling was achieved using the Pressure Implicit with Splitting of Operator (PISO) method, which is very effective in case of transient flows with large time steps. The method was able to give us accurate results even though we used a time step of 0.5 s.

The imposed criterion for convergence was that the scaled residuals of velocity should be below 0.001, and the scaled residuals of energy should be below 1×10^{-6}.

3.1. Grid independence

The mesh taken initially consists of structured quadrilateral elements. The grid is finer at the periphery to take care of the boundary layer effects.

Extensive grid independence tests were done. The grid was adapted several times in order to make the temperature and velocity gradients less than 10^{-7} s^{-1}. Successive adaptation of the grid led to results that were independent of grid. It may be mentioned that although a grid with 24 000 nodes was producing a satisfactory temperature profile in the static case, the stream functions were found to be grid dependent. A grid of 35 000 nodes was found to be satisfactory, the results remaining unchanged with a grid of 44 000 nodes.

Since rotating flows are found to be highly grid dependent, grid dependence tests were performed separately for the rotating case. In this case, a grid of 57 000 nodes was used. Since simulations at 15 rpm with a grid of 66 000 nodes did not produce any appreciable difference in flow

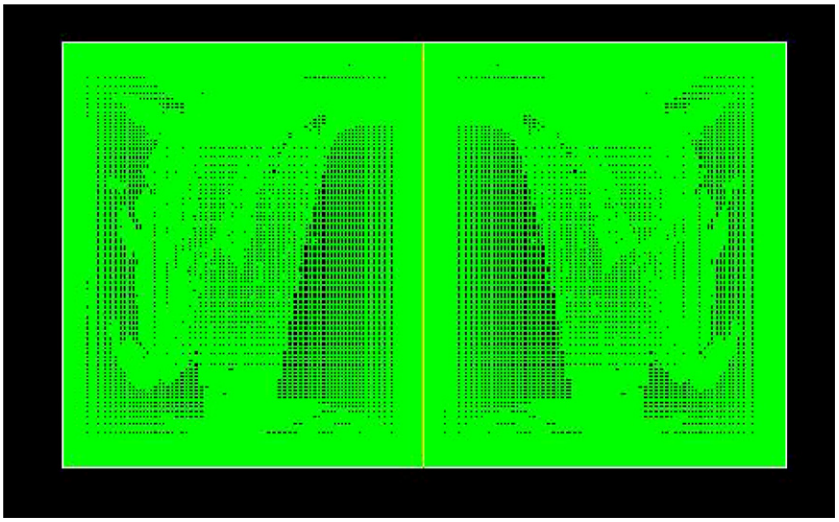

Fig. 2. The final adapted grid.

patterns, the grid with 57 000 nodes was found to be acceptable. The final adapted grid is shown in Fig. 2.

Simulations were done with a time step of 0.5 s and 0.1 s, which were in good agreement. Hence, a time step of 0.5 s was chosen.

4. Results and discussion

4.1. Validation

The simulation results have been validated with the results obtained by Datta et al. (1992). Here, the temperature distribution for natural convection in a cylinder of diameter 17 cm and height 10.1 cm, with a microwave radiation intensity of 1.125 W/cc has been considered. Fig. 3 illustrates the comparison between the experimental and computational results for the radial temperature profiles. Fig. 4 shows a comparison of the axial temperature profiles for various times. The predicted temperature profiles and experimental results (Datta et al., 1992) are in good agreement and the difference lies within 2.5 °C. Note that Datta et al. (1992) illustrate the temperature profiles in the absence of flow pattern. The flow pattern was validated with the results obtained by Franca and Haghighi (1996) for an identical problem using the adaptive finite element method. A comparison of the stream functions at 1 min and 3 min are shown in Fig. 5. The stream functions obtained with both these methods are in good agreement.

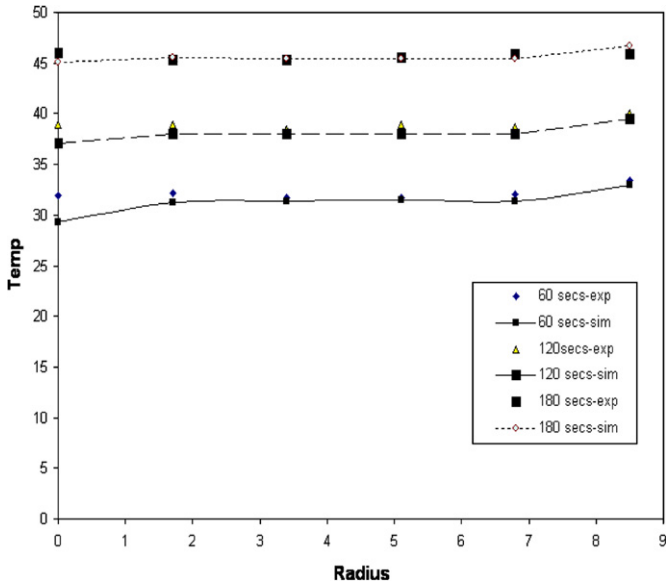

Fig. 3. Radial temperature at different times at $H = 6.8$ cm; comparison with experiment.

It is found in previous experimental study (Datta et al., 1992) that the turntable option was not turned on. But in practical applications of microwave heating, the container is generally placed in a turntable, whose rotation has a significant effect on temperature profiles.

4.2. Parametric study

In this section, the influence of three factors, conduction, natural convection due to gravitational forces, and flow due to rotation of the container, have been considered. Parametric study has been carried out to observe the effect of each of these factors separately and analyze their contributions in determining the heat transfer rate.

Hence, the following cases have been considered:

1. The pure conduction case, in the absence of gravity and rotation.
2. A rotation model without gravitational forces.
3. A natural convection case without rotation, which is our already validated result.

The temperature distribution as a function of time is plotted for all the cases in Fig. 6. As the temperature distributions in the cardinal directions show a monotonic

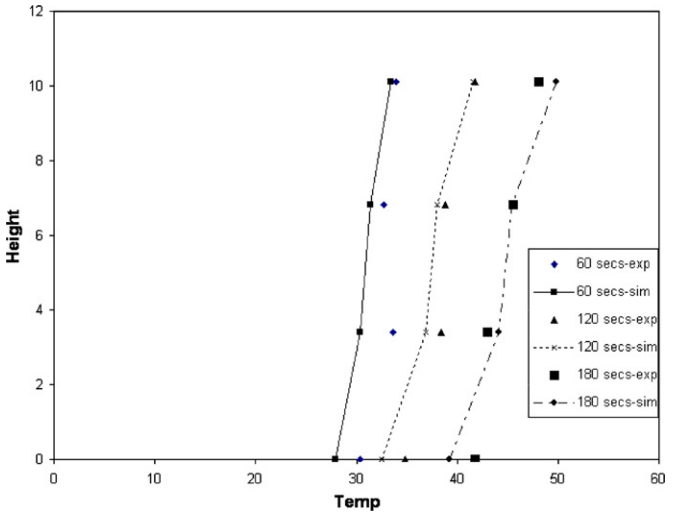

Fig. 4. Axial temperature profiles at $R = 5.1$ cm; comparison with experiment.

increase or decrease, the temperature range can also be taken as a measure of the density stratification.

As seen in Fig. 6, the first case is a conduction model, which is obtained by using the distributed parameter approach. The overestimation of the temperature range given by this model is attributed to the absence of mixing due to convection. Hence, we see that mixing due to convection plays an important role in achieving temperature uniformity in microwave driven convection.

In the second case, it may be expected that the temperature ranges would go down because of the flow, but the temperature ranges remain necessarily the same. The ratio of the centrifugal and Coriolis forces is given by $Ra_r/(Ta^{1/2}V)$, which is of the order of 10^{-3}. Thus we see that the centrifugal force is negligible at such low rotation rates and the flow is affected mainly due to the Coriolis force. Considering the swirl velocity to be the main velocity, the direction of the Coriolis force ($\hat{k} \times w$) acts towards the centre, pushing

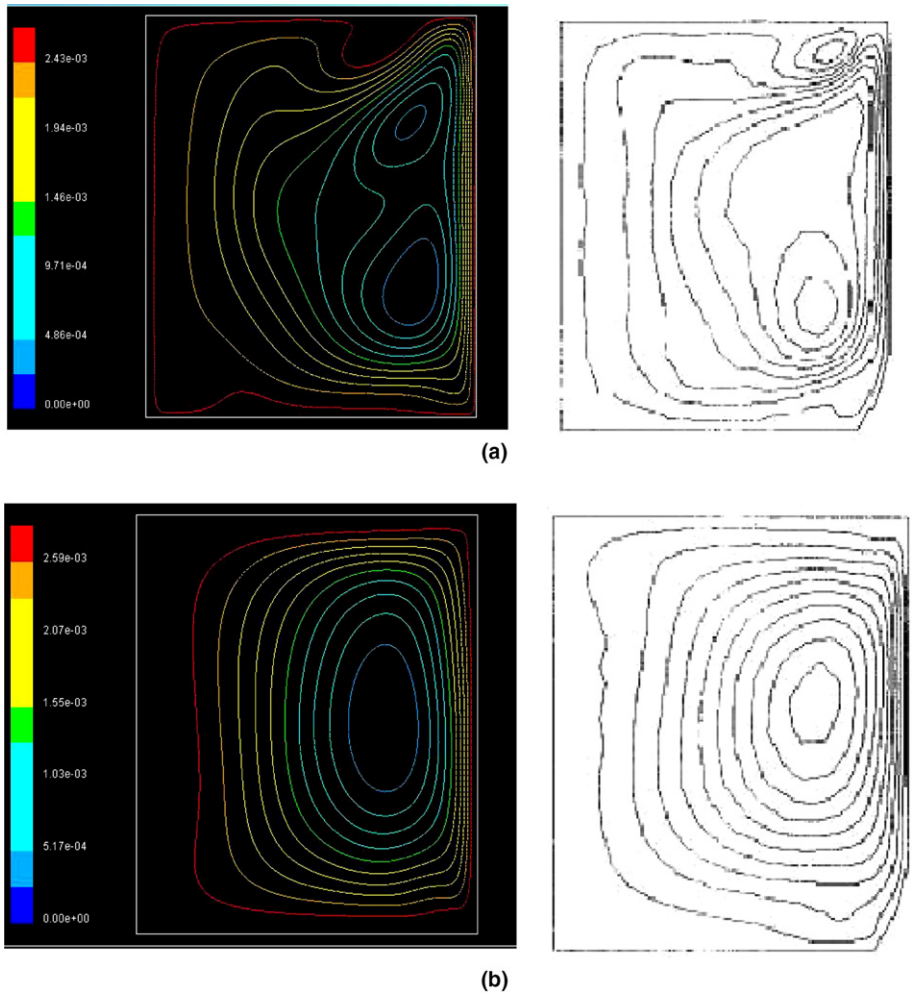

Fig. 5. Comparison of the stream functions obtained at (a)1 min and (b) 3 min (contours scaled in kg/s) [The patterns to the left are obtained by our simulations and those to the right are due to Franca and Haghighi].

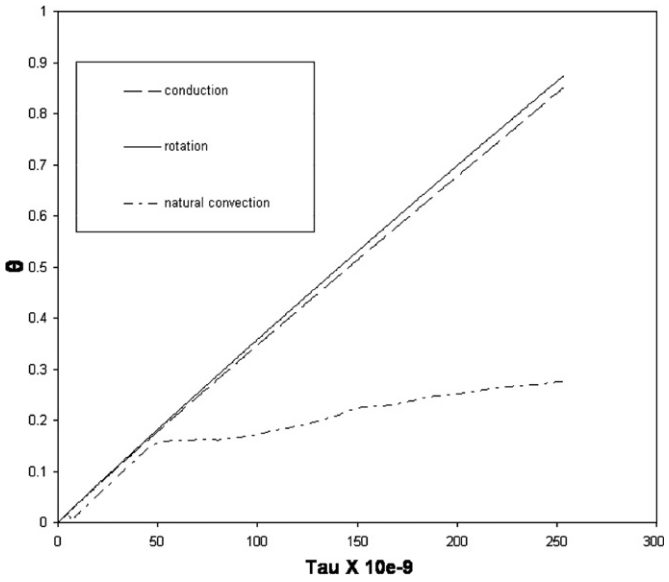

Fig. 6. Transient change in temperature ranges in all the three cases.

the denser fluid towards the core. Thus the lighter less dense fluid is pushed to the periphery, and this already heated fluid gets more heated, increasing the non-uniformities. Moreover, the flow in such cases is boundary layer driven, and hence the effects of flow induced mixing are essentially localized and do not affect the bulk region extensively, as in natural convection. Thus rotations at such slow rates do not cause a decrease in temperature range due to better mixing. On the other hand, in a configuration such as this, there is an increase in stratification. The effect of rotation is further investigated in the studies that follow. Fig. 7 shows the radial and axial velocity profiles. The radial velocity profiles show the formation of an Ekman boundary layer above and below, and the axial velocity profiles show a Taylor column in the central section, which is characteristic of rotation driven flow.

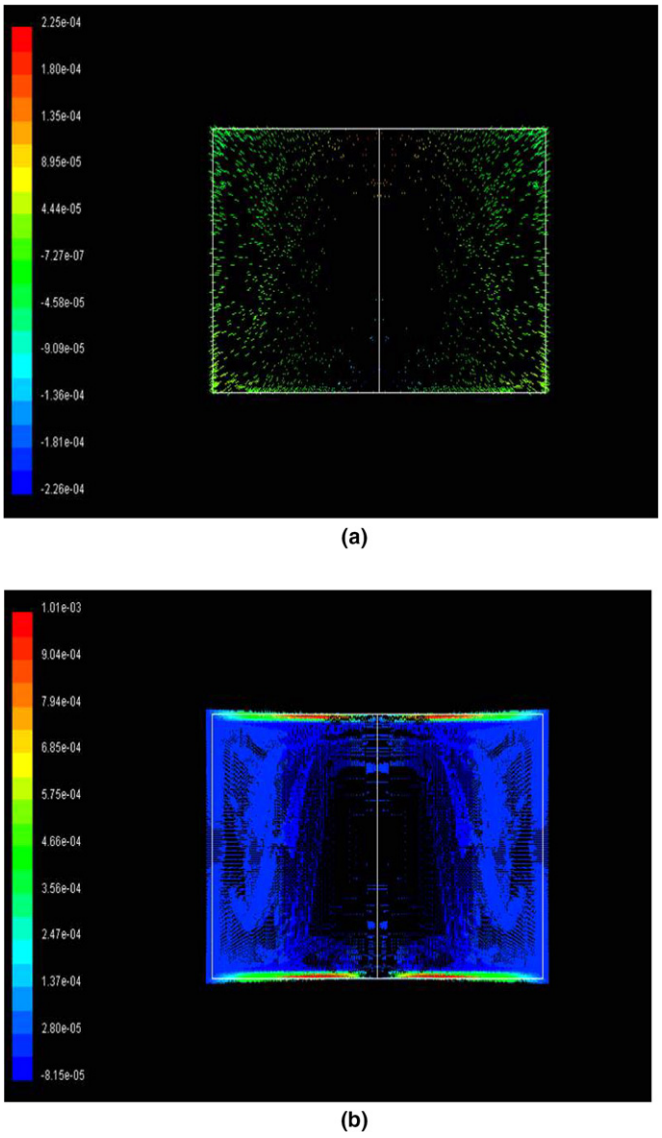

Fig. 7. Velocity profiles in the purely rotational case (a) axial and (b) radial.

4.3. Effect of rotation

In this section, the effect of rotation is exhaustively studied. Simulations are performed for five different rotation speeds, ranging from 3 rpm to 15 rpm, separately for three values of heat flux. The main forces affecting the flow can be found by a simple scaling analysis as before. The ratio of the centrifugal and the gravitational forces is given by the Froude number $Fr = \frac{\Omega^2 R}{g} = \frac{Ra_r}{Ra}$.

The Froude number values on the present analysis vary from 0.0008 to 0.02. Hence centrifugal effects can be neglected in relation to gravitational effects. As in Hamady et al. (1994), assuming the swirl velocity $w \sim Ra^{1/2}$, the ratio of the Coriolis and the gravitational forces is given as $(Ra/Ta)^{1/2}$.

In the current problem, $1.6 < (Ra/Ta)^{1/2} < 8.2$. Hence, the real interaction is between the Coriolis and gravitational forces. The effect of the Coriolis force in increasing stratification has been discussed earlier. The effect is very clear, as seen in Fig. 8. With the increase in Taylor number, the temperature non-uniformity is seen to increase monotonically. The Coriolis force pushes the heavier fluid to the centre, thus creating a static unheated central column, which is seen to increase with increase in angular velocity (Fig. 9). The heat transfer here is mainly through conduction, which is the least in these regions.

Another effect of the rotational forces is the emergence of secondary flows, driven by vertical pressure gradients. Rotation, in all cases leads to such secondary flows, as noted by Prud'homme, Hung Nguyen, and Mao (1993). The presence of such secondary flows can be clearly seen from the stream function profiles in Fig. 10. In the static case, the well known Benard convection pattern consisting of a pair of counter-rotating cells is observed. Rotation introduces a secondary flow, which leads to the creation of vortices. As the circulating fluid gets diverted into these localized vortices, the strength of the main circulation

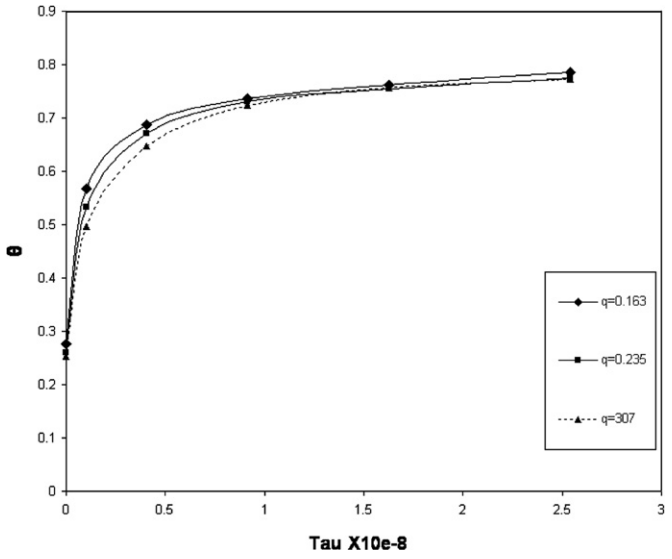

Fig. 8. Increase in temperature non-uniformities with Taylor number.

decreases, thereby reducing natural convection. This fact is clearly brought out in Fig. 11. The decrease in axial velocities clearly signifies a reduction in the strength of the main circulation due to natural convection. Such reductions on heat transfer due to rotational effects have been noted previously in literature. Hide and Mason (1975) found that for a rotating cylindrical annulus, Nusselt number is proportional to $\Omega^{-1/2}$.

Hence it may be noted that contrary to expectation, rotation causes a greater non-uniformity of temperature in the present case.

4.4. Effect of power source intensity

Changes in power source intensity significantly influence temperature distributions and flow profiles. Studies have been made over a wide range of power source distributions in order to arrive at certain important conclusions.

A study of the temperature profiles reveal that increasing the power source intensity leads to greater power being conducted to the centre, and hence a decrease in the height of the previously mentioned central column, as seen in Fig. 12.

Transient temperature profiles in different simulations (Fig. 13) show an apparent linearity. But, mathematically linearity cannot be strictly proved, as shown in Prosetya and Datta (1991), since linearity implies that on performing a linear regression analysis, the actual data points must lie either on the regression line, or must be distributed approximately equally on both sides of the regression line, without any particular bias. Regression analysis in our case indicated certain trends and hence, a strict linearity cannot be established. But, however, as in Prosetya and Datta (1991), we observe that for all practical purposes linearity may be assumed with little loss of accuracy. A rigorous regression analysis is carried out to arrive at this fact.

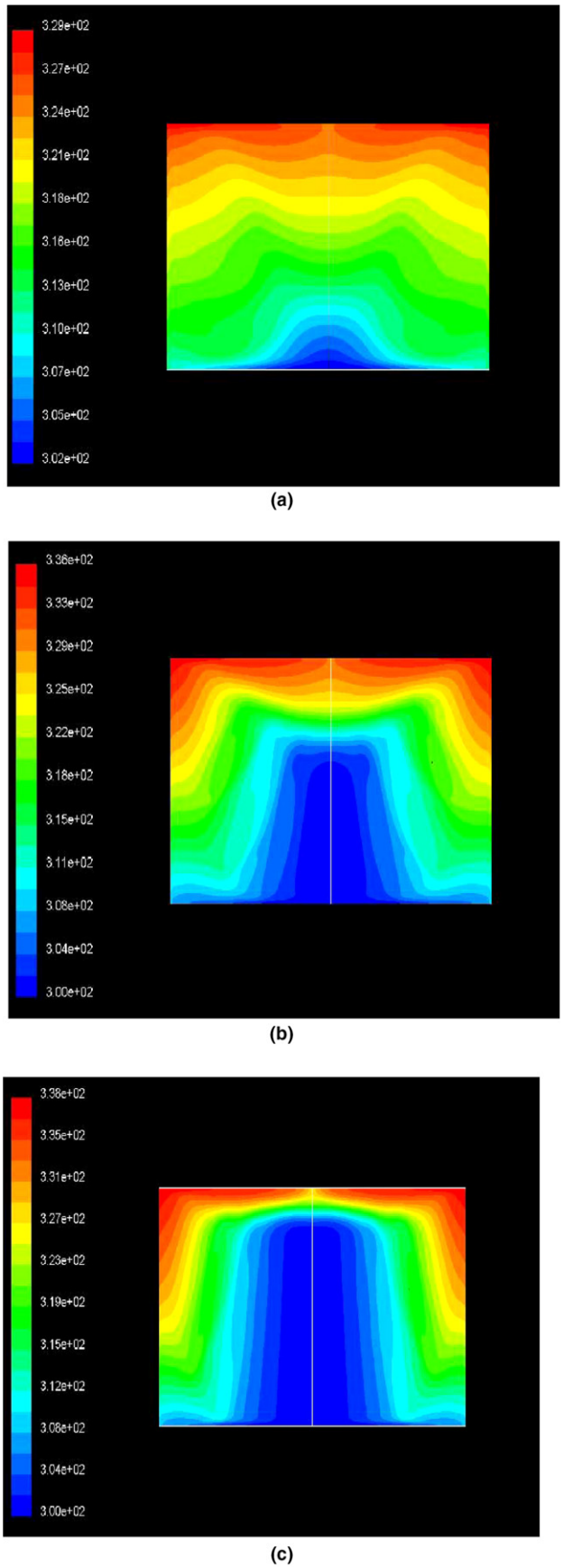

Fig. 9. Temperature profiles in (a) static case, (b) 3 rpm and (c) 15 rpm.

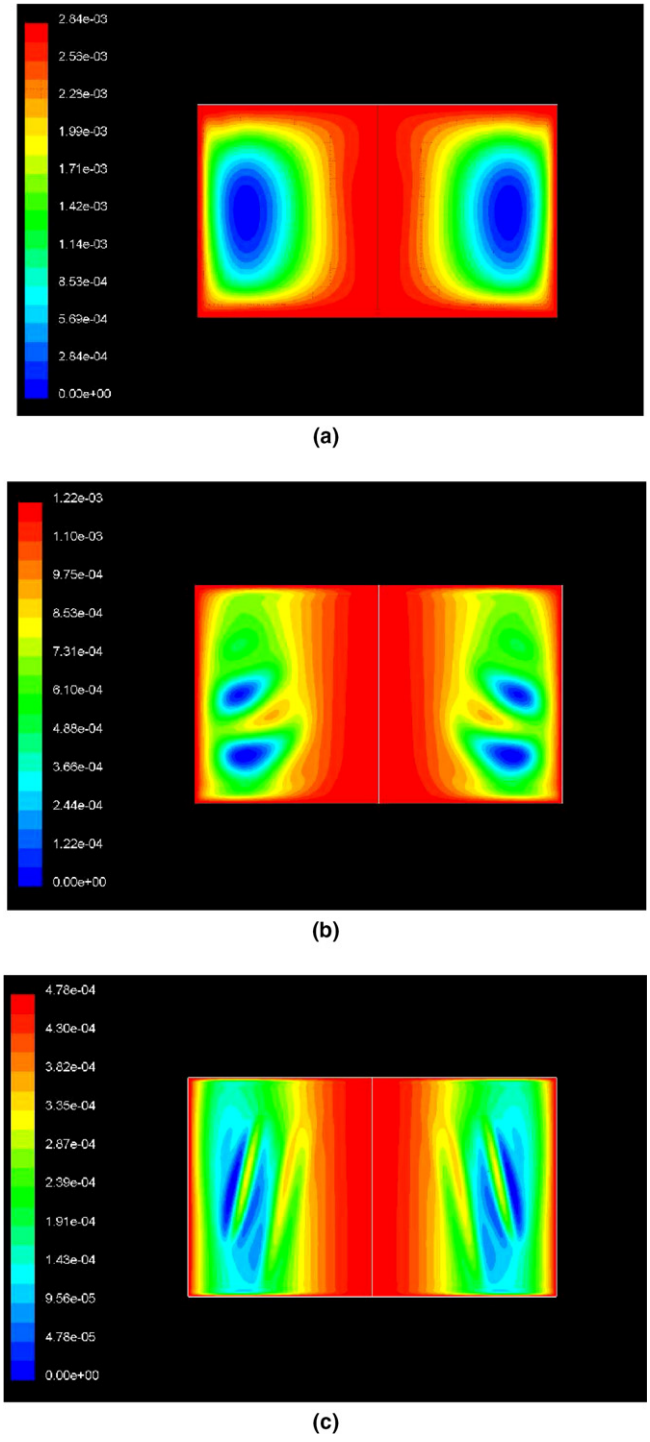

Fig. 10. Stream function profiles at (a) static case, (b) 3 rpm and (c) 15 rpm.

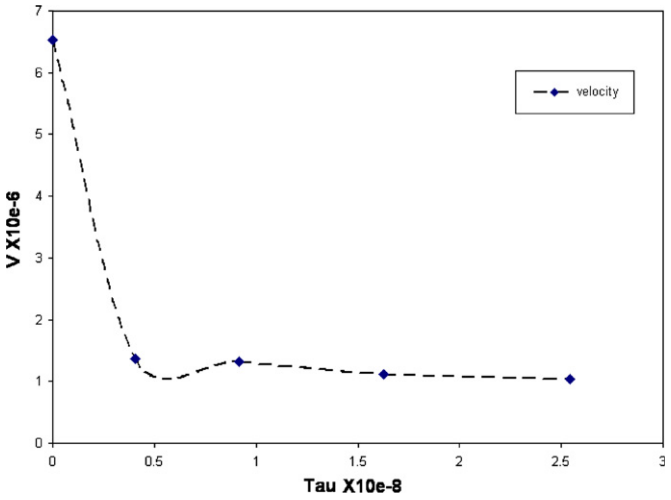

Fig. 11. Change in minimum axial velocities with angular velocity.

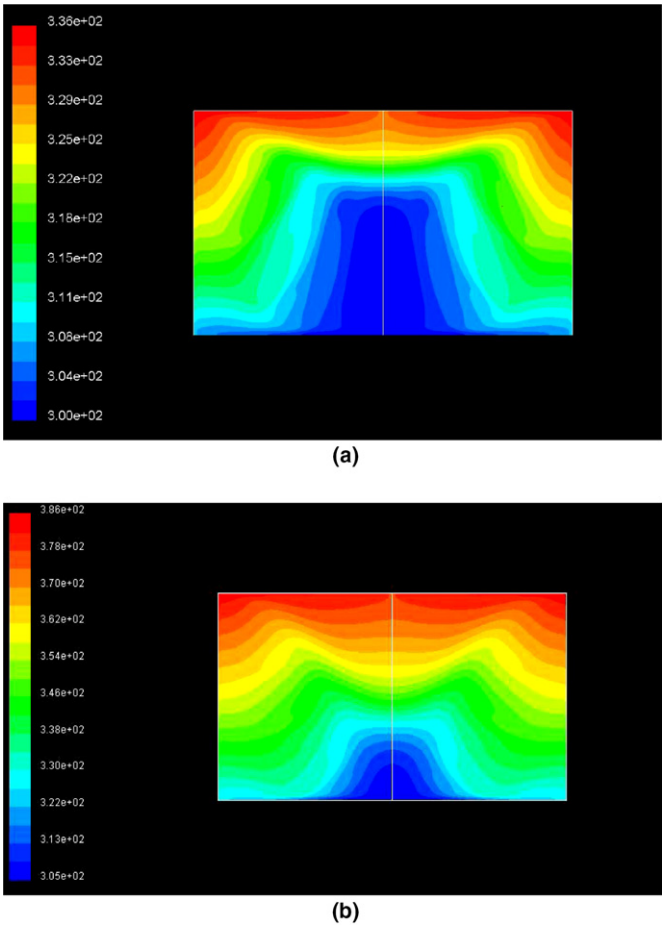

Fig. 12. Temperature profiles at (a) $q = 0.1627$ and (b) $q = 0.3796$.

The merit of the fit is given by the coefficient of determination R^2 (Sachs, 1984).The closer the R^2 values are to 1, the better the correlation. The R^2 values in Table 1 reveal that linearity can be assumed for all practical purposes.

With such an assumption of linearity, we have, for the first time, tried to arrive at a generalized correlation that describes transient changes in average temperatures. Since the correlation involves only non-dimensional parameters, it can be effectively used for different situations.

Simulations have been performed for several values of power source intensity (Table 1). The straight line fits have been obtained in each case.. As the R^2 values indicate, the deviation from linearity is small. In each case, the profile

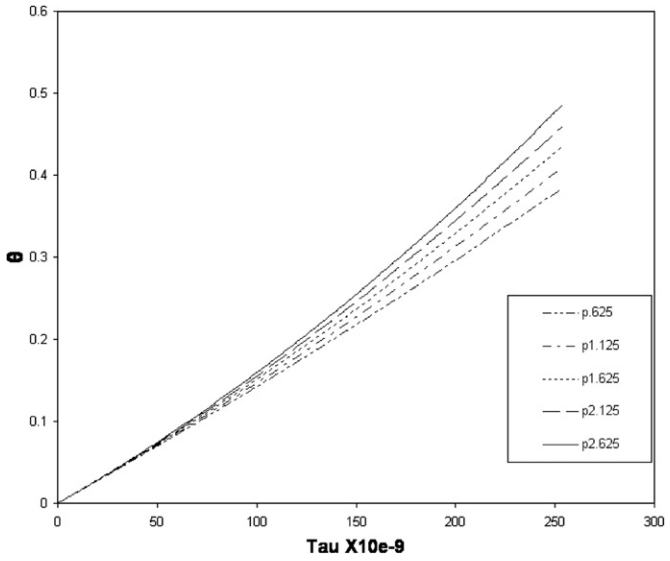

Fig. 13. Transient changes in average temperatures for various values of power.

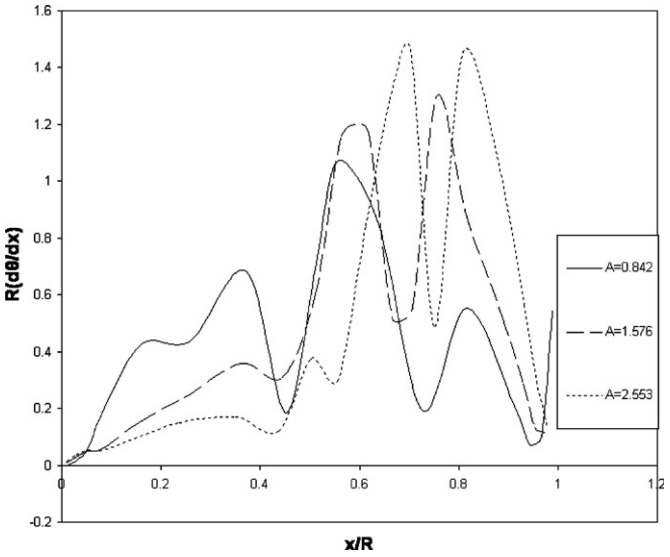

Fig. 14. Spatial derivatives of temperature range for various aspect ratios, taken at the mid-plane.

Table 1
Temperature derivatives and R^2 values for different values of power source intensity

Q_0	q	$d\theta/d\tau \times 10^{11}$	R^2
0.375	0.0542	0.1453	0.9998
0.625	0.0904	0.1512	0.9993
0.875	0.1265	0.1563	0.9990
1.125	0.1627	0.1615	0.9985
1.375	0.1989	0.1673	0.9978
1.625	0.2350	0.1717	0.9974
1.875	0.2712	0.1766	0.9969
2.125	0.3073	0.1814	0.9964
2.375	0.3435	0.1862	0.9958
2.625	0.3796	0.1915	0.9949

being linear, only the slopes of the straight lines change with change in power source intensity. Since the energy equation does not involve q, ideally one does not expect the temperature–time profile to change with power intensity. These changes occur because of the coupled nature of the equation, as also noted by Prosetya and Datta (1991).This complex coupling of the equations make any further analysis impossible. However, for all practical purposes, the following correlation can be used.

$$\frac{\partial\theta}{\partial\tau} \times 10^{11} = 0.1401q + 0.1385 \tag{25}$$

Note that the fit is purely empirical, and has been done solely based on statistical consideration. But considering that the R^2 value for the fit is 0.999, the correlation may be used for all practical purposes with little loss of accuracy.

4.5. Effect of aspect ratio

It is also interesting to note the effect of change in the aspect ratio. Since the power is volumetrically distributed, effort must be taken to see that the power remains constant as the aspect ratios are changed. The total power is

$$Q = 2\pi h Q_0 \delta^2 \left[\frac{R}{\delta} - 1 + \exp\left(\frac{-R}{\delta}\right)\right] \tag{26}$$

Taking an average value of δ over the temperature range, we calculate the dimensions so as to keep the power constant. There are no remarkable changes in the overall temperature range, but the spatial derivatives of temperature (Fig. 14) in the unheated central region ($x/R = 0$–0.4) are seen to decrease significantly as the as the aspect ratio $A(=R/h)$ was increased. This clearly shows the decrease in conduction to the central layers with the increase in aspect ratio. Thus to decrease the width of a central unheated zone, and prevent an increased localization of power in the peripheral region, the aspect ratio should be kept at a minimum. It is to be noted that tests with an aspect ratio less than that in the experiment were not performed since the validity of the Lambert's law in such regions is not ascertained. We may conclude from such observations that in the regime where the Lambert's law is valid, the aspect ratio should be kept as low as possible.

5. Conclusion

A numerical study is carried out to observe the effects of container rotation in the case of the microwave heating of containerized liquids. The solution procedure is validated with experimental results of natural convection in microwave heating available in literature. Subsequently, a detailed parametric study is carried out, and the following conclusive remarks may be made:

1. In case of a symmetric microwave source, preferably rotation should not be given, since it serves only to increase the non-uniformity of temperatures. Even in

the case of a non-uniform source, the rate of rotation should be controlled, keeping in mind that increases rotation rates lead to an increased volume of unheated central region. Such effects can be countered by increasing the power source intensity.

2. For all practical purposes, the time-temperature graph remains linear, and the time evolution of temperature can be correlated with increase in power source intensity in a linear fashion.
3. The aspect ratio must be kept as low as possible, in the regime where the Lambert Law assumption is supposed to be valid, in order that the heat be conducted effectively to the central regions.

Acknowledgements

The authors would like to express their gratitude to Prof. A.K Datta (Professor, Biological and Bio Environmental Engineering, Cornell University) for providing us with a copy of his paper (Datta et al., 1992), which was of invaluable help to us.

References

Ayappa, K. G., Brandon, S., Derby, J. J., Davis, H. T., & Davis, E. A. (1994). Microwave driven convection in a square cavity. *AICHE Journal, 40*(7), 1268–1272.

Ayappa, K. G., Davis, H. T., Crapiste, G., Davis, E. A., & Gordon, J. (1991). Microwave heating: an evaluation of power formulations. *Chemical Engineering Science, 46*, 1005–1016.

Basak, T., & Ayappa, K. G. (2001). Influence of internal convection during microwave thawing of cylinders. *AICHE Journal, 47*, 835–850.

Boubnov, B. M., & Golitsyn, G. S. (1986). Experimental study of convective structures in rotating fluids. *Journal of Fluid Mechanics, 167*, 503–531.

Boubnov, B. M., & Golitsyn, G. S. (1995). *Convection in rotating fluids*. Dordrecht, Holland: Kluwer Academic Publishers.

Datta, A. K., Prosetya, H., & Hu, W. (1992). Mathematical modeling of batch heating of liquids in a microwave cavity. *Journal of Microwave Power and Electromagnetic Energy, 27*(1), 38–48.

Franca, A. S., & Haghighi, K. (1996). Adaptive finite element analysis of microwave driven convection. *International Communications in Heat and Mass Transfer, 23*, 177–186.

Hamady, F. J., Lloyd, J. R., Yang, K. T., & Yang, H. Q. (1994). A study of natural convection in a rotating enclosure. *ASME Journal of Heat Transfer, 116*, 136–143.

Hide, R., & Mason, P. J. (1975). Sloping convection in a rotating liquid. *Advances in Physics, 24*(1), 47–100.

Hudson, J. L., Tang, D., & Abell, S. (1978). Effects of centrifugally driven thermal convection on rotating cylinders. *Journal of Fluid Mechanics, 86*, 147–159.

Lenz, R. R. (1980). On the microwave heating of saline solutions. *Journal Of Microwave Power, 15*(2), 107–111.

Le Van, Q., & Gourdenne, A. (1987). Micowave curing of epoxy resins with Diaminodiphenylmethane: I. *General Features of European Polymer Journal, 23*, 777–780.

Malaczynski, G. W. (1988). Adhesive processing by electromagnetic irradiation. *Polymer Engineering and Science, 28*, 1270–1274.

May, H. O. (1991). A numerical study of natural convection in an inclined square cavity enclosure containing internal heat sources. *International Journal of Heat and Mass Transfer, 34*, 919–928.

Prosetya, H., & Datta, A. K. (1991). Batch microwave heating of liquids: An experimental study. *Journal of Microwave power and Electromagnetic Energy, 26*(14), 215–226.

Prud'homme, M., Hung Nguyen, T., & Mao, P. G. (1993). Numerical simulation of melting inside a rotating cylindrical enclosure. *International Journal of Heat and Mass Transfer, 48*, 57–69.

Ratanadecho, P., Aoki, K., & Akahori, M. (2002). A numerical and experimental investigation of the modeling of microwave heating for liquid layers using a rectangular wave guide (effects of natural convection and dielectric properties). *Applied Mathematical Modelling, 26*, 449–472.

Roschina, N. A., Uvarov, A. V., & Osipov, A. I. (2005). Natural convection in an annulus between coaxial horizontal cylinders with internal heat generation. *International Journal of Heat and Mass Transfer, 48*, 4518–4525.

Rossby, H. T. (1969). A study of benard convection with and without rotation. *Journal of Fluid Mechanics, 36*, 309–335.

Sachs, Lothar (1984). *Applied statistics – A handbook of techniques*. New York: Springer-Verlag.

Saltiel, C., & Datta, A. K. (1999). Heat and mass transfer in microwave processing. *Advances in Heat Transfer, 33*, 1–94.

Sutton, W. S. (1989). Microwave processing of ceramic materials. *Ceramic Bull., 68*, 376–386.

Tasaka, Y., & Takeda, Y. (2005). Effect of heat source distribution on natural convection induced by internal heating. *International Journal of Heat and Mass Transfer, 48*, 1164–1174.

Wei, C. K., Davis, H. T., Davis, E. A., & Gordon, J. (1985). Heat and mass transfer in water laden sandstone: Microwave heating. *AICHE Journal, 31*, 842–848.

Yang, H. W., & Gunasekaran, S. (2004). Comparison of temperature distribution in model food cylinders based on Maxwell's equations and Lambert's law during pulsed microwave heating. *Journal of Food Engineering, 64*, 445–453.

Zhang, Q., Jackson, T., & Ungan, A. (2000). Numerical modeling of microwave induced natural convection. *International Journal of Heat and Mass Transfer, 43*, 2141–2154.